MODELLING OF GASEOUS PHASE IN BUBBLE COLUMNS

Jana VAŠÁKOVÁ and Jan ČERMÁK

Institute of Chemical Process Fundamentals,
Czechoslovak Academy of Sciences, 165 02 Prague 6-Suchdol

Received October 2, 1990
Accepted November 5, 1990

An axial dispersion model of a bubble column was verified by an experimental method based on pseudo-random binary signals of maximum length. The diameter of the column was 0·292 m and the height of the dispersion layer was 1·33 m. Water formed a stagnant liquid layer and a mixture of air with up to 5 vol. % of CO_2 formed a streaming gas phase. The model was evaluated from the response of the bubble column to pseudo-random binary signals and from impulse characteristics calculated from this response by the correlation method. The use of the axial dispersion model with mass transfer was evaluated in dependence on the driving force.

Bubble columns are often used in chemical industry, e.g. in organic technology, pharmaceutical industry, and in biotechnology. Most of the relevant studies are concerned with the description of characteristic parameters of bubble columns or with correlation equations for the estimation of these quantities from experimental data. The present work brings results attained during verification of an axial dispersion model of bubble column using the method of pseudo-random binary signals of maximum length (PRBS). The bubble column was compared with its model on the basis of impulse characteristics determined from the response of the system to PRBS. This is advantageous since the calculation of the impulse characteristic is simplified owing to certain special properties of PRBS. The PRBS method can be employed even if some model parameters are subject to noise. This circumstance is important in the case of bubble columns, since processes taking place in them are stochastic in nature. The present work is concerned with the study of the gaseous phase, which has been studied up to now to a lesser extent than the liquid phase.

THEORETICAL

Properties of PRBS

A pseudo-random binary signal of maximum length[1-6] is a determined periodic signal acquiring only two values which are symmetrical with respect to zero. Transitions between the two values take place at intervals which are whole multiples of a basic time interval, Δt. Thus, the pseudo-random binary series repeats itself peri-

odically, after $N\,\Delta t$, where N is called the PRBS period (e.g. $N = 15$ in Fig. 1), which should be equal to $2^n - 1$, where n is an integer. Generation of PRBS is effected by means of shift registers with a feedback[6]. The mathematical description of the feedback circuit expressed by a difference equation forms a basis for programmed generation of PRBS. The most important property of PRBS is the form of its pseudocorrelation function, $R_{xx}(j\,\Delta t)$:

$$R_{xx}(j\,\Delta t) = \begin{cases} \bar{a}^2, j = 0, N, 2N, \ldots \\ -\bar{a}^2/N, j \neq 0, N, 2N, \ldots \end{cases} \tag{1}$$

In practical applications, however, the starting signal is distorted by the influence of ADC converters. The distortion can be linear, exponential, or combined linear and exponential.

Model of the Bubble Column

The flow of phases in a real bubble column is not ideal; it is usually described by stage or dispersion models. The former are based on the concept of separate flow regions joined either in series or in parallel, the latter on the analogy between the mechanism of stirring in the real flow and diffusion. For the single stage bubble column used by us, the one-dimensional dispersion model of Mangartz and Pilhofer[22] was selected from the literature[7-23]. The model equations for both the gaseous and liquid phases were derived from the mass balance in a bubble column in the non-stationary state[24]. The gas phase is described by the equation (2)

$$\frac{\partial c_g}{\partial t} = D_g \frac{\partial^2 c_g}{\partial z^2} - U \frac{\partial c_g}{\partial z} - \frac{k_l a_l (1 - \varepsilon_g)}{\varepsilon_g} (\chi c_g - c_l) \tag{2}$$

and the perfectly stirred, stationary liquid phase by the equation (3)

$$\frac{\partial c_l}{\partial t} = k_l a_l \left(\chi \frac{1}{L} \int_0^L c_g \, \mathrm{d}z - c_l \right). \tag{3}$$

The boundary conditions are given as

$$z = 0: Uc_i = Uc_g - D_g \frac{\partial c_g}{\partial z} \tag{4}$$

$$z = L: \frac{\partial c_g}{\partial z} = 0 \tag{5}$$

and the initial conditions

$$t = 0: c_g = c_{g1}, c_l = c_{l1} . \qquad (6), (7)$$

Equations (2) and (3) with the conditions (4)–(7) represent the axial dispersion model with mass transfer. If the balanced constituent is insoluble in the liquid phase, the last term in Eq. (2) is equal to zero and we obtain the equation

$$\frac{\partial c_g}{\partial t} = D_g \frac{\partial^2 c_g}{\partial z^2} - U \frac{\partial c_g}{\partial z} \qquad (8)$$

which describes the axial dispersion model without mass transfer. The boundary conditions are equations (4) and (5) besides the initial condition (6). For the numerical solution, the following dimensionless parameters were introduced:

$$c_g^* = \frac{c_g - c_{g1}}{c_{g2} - c_{g1}} , \quad c_l^* = \frac{c_l - c_{l1}}{c_{l2} - c_{l1}} , \qquad (9), (10)$$

$$t^* = tU/L, z^* = z/L. \qquad (11), (12)$$

Solution of Model Equations for PRBS

The equations for the axial dispersion model with mass transfer, (2) and (3), and without mass transfer, (8), can be solved for various input signals. For example, if the inlet concentration c_i in the boundary condition (4) is changed according to a step function, the response of the model corresponds to a transient characteristic. In calculating the model response to a pseudo-random binary input signal, we proceeded in a similar way. The concentration c_i in Eq. (4) was changed in accord with a chosen PRBS. The obtained model responses were then used to calculate impulse characteristics by the correlation method, based on the Wiener–Hopf equation (13), which represents a dynamic coupling between autocorrelation function of the input signal, crosscorrelation function of the input and output signals, and impulse characteristic:

$$R_{xy}(\tau) = \int_0^\infty h(t)\, R_{xx}(\tau - t)\, \mathrm{d}t . \qquad (13)$$

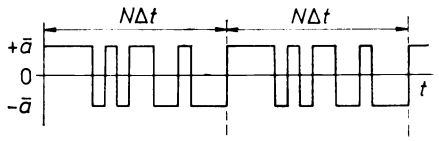

FIG. 1

Dependence of PRBS on time: $+\bar{a}$ upper level of PRBS, $\bar{a}$ lower level of PRBS, Δt basic time interval, N period of PRBS

When PRBS is used as input signal, this equation is replaced by Eq. (*14*), in which the summation stands for the integral, the pseudocorrelation function stands for the correlation function, and g_i corresponds to the area under the impulse characteristic delimited by its i-th ordinate, and the time interval Δt:

$$R_{xy}(j\,\Delta t) = \frac{1}{N}\sum_{i=0}^{N-1} g_i R_{xx}[(j-i)\,\Delta t] + \frac{1}{N}\sum_{i=0}^{N-1} g_i R_{xN}[(j-i)\,\Delta t]\,, \qquad (14)$$

where $j = 0, 1, \ldots N-1$. The pseudocorrelation function $R_{xN}[(j-i)\,\Delta t]$ expresses the correlation of the input signal and the noise added to the output signal. Assuming a system with non-correlated noise, we obtain by successive rearrangements of Eq. (*14*) the ordinates of the impulse characteristic (use was made of equations (*15*) and (*16*))

$$h(0) = \frac{2}{\Delta t \bar{a}^2}\frac{N}{N+1}\left[R_{xy}(0) + \sum_{j=0}^{N-1} R_{xy}(j\,\Delta t)\right], \qquad (15)$$

$$h(i\,\Delta t) = \frac{1}{\Delta t \bar{a}^2}\frac{N}{N+1}\left[R_{xy}(i\,\Delta t) + \sum_{j=0}^{N-1} R_{xy}(j\,\Delta t)\right], \qquad (16)$$

where $i = 1, 2, \ldots N-1$. The pseudocorrelation function $R_{xy}(k\,\Delta t)$ was calculated as

$$R_{xy}(k\,\Delta t) = \frac{1}{N}\sum_{i=0}^{N-1} x[(i-k)\,\Delta t]\, y(i\,\Delta t)\,. \qquad (17)$$

EXPERIMENTAL

Parameters of PRBS

The basic PRBS parameters are selected according to the system under study, experimental possibilities, and frequency properties of PRBS. The length of the period should be such that the period at least involves the response of the system to one of the basic input functions. The period N is also related with the frequency properties of PRBS, which can be followed by amplitude-frequency spectra[25]. Their calculation shows that the efficient frequency band of ideal PRBS is limited from below by the frequency $1/N\,\Delta t$. The upper limiting frequency of the band depends on the experimentator's choice. The efficient frequency band of distorted PRBS is delimited in the same manner. The basic time interval Δt is chosen according to the time constants of the apparatuses used for the measurement of PRBS or of the response of the system to PRBS. From this point of view, the apparatus with the highest time constant is critical. The interval Δt should be at least ten times longer than this time constant. It follows from the above discussion that the values of N and Δt are interrelated and hence one of them cannot be chosen without regard to the other.

Description of the Apparatus

The experimental set-up is shown schematically in Fig. 2; it was also used in earlier measurements[24]. A single-stage bubble column 1 was provided with a distributor plate 2 and a pre-distributor plate 4 in a cylindrical steel chamber 3. Both plates were made of brass, they were 3 mm thick and had 0·2% of free surface area. A CO_2/air mixture was led to below the pre-distributor plate. The air was taken from a pressurized air supply 5 through reduction valve 6, needle valve 7 and rotameter 8. Carbon dioxide was taken from pressure cylinder 9 through reduction valve 10, needle valve 11 and rotameter 12. After leaving the rotameters 8 and 12 a constant flow of CO_2 or air was alternately added to the mixture. The air was again taken from the supply 5, led through reduction set-up 13, needle valve 14, solenoid valve 15, and rotameter 16. Carbon dioxide was led similarly from pressure cylinder 9 through reduction valve 17, needle valve 18, solenoid valve 19, and rotameter 16. Alternate opening of the solenoid valves was controlled by a generator of the type PSG-1 (denoted as G) with a contact-less switch SW. The two solenoid valves were arranged in such a way that in the closed state the gas flow rate through valves 20 and 21 into the air atmosphere were the same. The valves 20 and 21 were opened so that they had the same resistance against gas flow as the remaining gas conducts. In this way the pressure shocks during opening the solenoid valves were damped.

Behind the rotameter 22 the gas mixture proceeded through the water led into the column from the water tap through valve 23. The column was closed with a stainless steel lid combined with organic glass 24, on whose inner side a mesh with Raschig rings 25 was fastened. The rings prevented loss of water drops through the steel tube outlet of 15 mm inner diameter mounted in the center of the lid. The tube was led into column 26 filled with water. The resistance of the water column caused an overpressure in the gas stream coming out from the bubble column; the gas was fed into the analyser, whose correct functioning was conditioned by the overpressure.

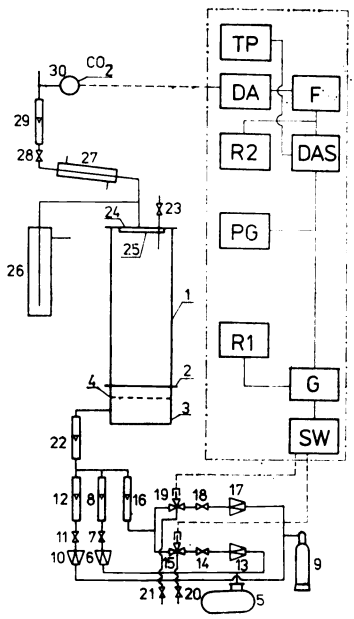

FIG. 2

Scheme of apparatus: 1 bubble column; 2 distributor plate; 3 steel chamber; 4 pre-distributor plate; 5 compressed air reservoir; 6, 10, 17 reduction valves; 7, 11, 14, 18, 28 needle valves; 8, 12, 16, 22 rotameters; 9 pressure cylinder; 13 reduction set-up; 15, 19 solenoid valves; 20, 21, 23 valves; 24 lid of column; 25 mesh with Raschig rings; 26 small column filled with water; 27 cooler; 29 flow regulator; 30 IR analyser URAS; G generator PSG-1; SW contact-less switch; R1, R2 pen recorders; PG pulse generator; DAS data acquisition system R 546; F tunable filter RFT; DA differential amplifier; TP tape puncher

A side tube of 5 mm inner diameter was mounted on the steel tube 30 mm above the lid; the small tube served to lead the gas mixture into cooler 27 in which water vapour was removed from the gas. This was then led through flow regulator 29 into a URAS type IR analyser 30, whose symmetrical electrical signal was converted by an NA2 type differential amplifier DA and a tunable filter RFT F to an asymmetrical signal. This was led to data acquisition system R 546 DAS and finally recorded on a punched tape. Synchronous functioning of the PSG-1 generator and of the data acquisition system was therefore controlled by pulse generator PG.

Obtaining the Data

Before the measurement itself, a series of the input pulses was recorded to estimate their distortion parameters. After adjusting the CO_2 concentration corresponding to the lower and upper levels of PRBS, the transient characteristic was measured in both directions. Then the response of the bubble column on PRBS at $N = 7$ and $\Delta t = 16$ s was measured as the output signal, and the output of the PSG-1 generator was measured as the input signal. The experiment was repeated for PRBS of chosen parameters, $N = 31$ and $\Delta t = 16$ s. The flow of gas through the column was 1·67 $dm^3\ s^{-1}$, the flow of water was equal to zero. The height of the dispersion layer was 1·33 m and the flow of the measured gas through the analyser 8·33 $cm^3\ s^{-1}$. The CO_2 concentrations of the lower and upper level of PRBS were in turn 4 and 5 vol. %, 1 and 2 vol. %, and 1 and 5 vol. %, respectively.

RESULTS

The absorption and desorption of CO_2 from the gas mixture to water in the bubble column was described by the axial dispersion model with mass transfer, Eqs (*2*)–(*7*). The model parameters were: column diameter 0·292 m, height of dispersion layer 1·33 m, superficial gas velocity 0·0249 m s^{-1}, gas hold-up 0·08 (ref.[26]), $k_l a_l =$ $= 0{\cdot}0258\ s^{-1}$ (ref.[27]), and gas dispersion coefficient 0·0454 $m^2\ s^{-1}$ (ref.[22]). The Henry constant, necessary for the calculation of the linear equilibrium coefficient χ,

$$\chi = RT/H\,, \tag{18}$$

was given as function of the column temperature.

Distortion Parameters of PRBS

The distortion parameters of PRBS were evaluated by nonlinear regression of the transient characteristic data using the measured CO_2 concentrations 1·24 and 5·17 vol. % for the lower and upper levels, respectively, at an amplification of the differential amplifier equal to 1. In the dimensionless form, the calculated slope of the linearly distorted pulse section was equal to 0·209, its height 0·500, and the time constant of the exponentially distorted portion 1·682 (compare Fig. 3).

Responses of the Bubble Column to PRBS

The responses of the column to input PRBS were compared with the responses of

the model. An experiment for $N_{PRBS} = 7$ and $\Delta t = 16$ s is illustrated in Fig. 4, where the solid line shows the model response, circles correspond to measured values, and the dashed lines delimit the errors. The experimental errors involved contributions from the data acquisition system and from the noise. The experimental parameters are given in the first line of Table I. In Fig. 5 are shown three periods of the experiment whose data are in the second line of Table I. The experiments were recorded after decay of the transition process due to different numbers of zeros and units in PRBS. The calculated values were recorded after 1 s, the measured ones after 2 s.

Impulse Characteristics

The measured and calculated data for $N_{PRBS} = 31$ were also compared by using the impulse characteristics. Under certain assumptions, it is possible to derive a relation for the calculation of the correction factor[28-30] by which the impulse characteristic of the system with distorted input PRBS differs from that with an ideal PRBS. Since the PRBS used did not satisfy the mentioned assumptions and no other method of estimation of the correction factor was found in the literature, the impulse characteristics were compared without determining the correction factor. The results were, however, not impaired since the correction factor was the same for all impulse characteristics.

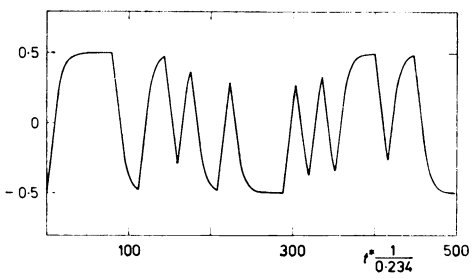

FIG. 3

Dependence of distorted PRBS on dimensionless time: $N_{PRBS} = 31$, $\Delta t = 16$ s

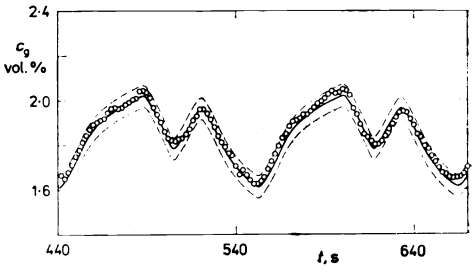

FIG. 4

Dependence of CO_2 concentration in the exit gas on the time. Approximately two periods are shown for $N_{PRBS} = 7$ and $\Delta t = 16$ s. The lower and upper levels of PRBS correspond to 1·25 and 2·28 vol. % of CO_2, respectively; ——— calculated, o measured values, — — — limits of errors

In Figs 6 and 7 are shown the impulse characteristics corresponding to the experiments whose parameters are in the second and third lines of Table I, respectively. The impulse characteristics were calculated from dimensionless input and output signals, recorded every 16 s, i.e. at time intervals corresponding to Δt_{PRBS}. In the case of the experimental input signal, distorted PRBS was assigned to the recorded ideal PRBS of the PSG-1 generator.

TABLE I

Response of the column to input PRBS

CO_2, vol. %[a]	CO_2, vol. %[b]	N[c]	t, s[d]	DA[e]	T, K[f]
1·25	2·28	7	16	2	288·75
4·13	5·02	31	16	1	288·85
1·22	5·17	31	16	1	288·65

[a] Measured concentration of lower level of PRBS, [b] measured concentration of upper level of PRBS, [c] period of PRBS, [d] time constant of PRBS, [e] amplification of differential amplifier, [f] temperature of water in column.

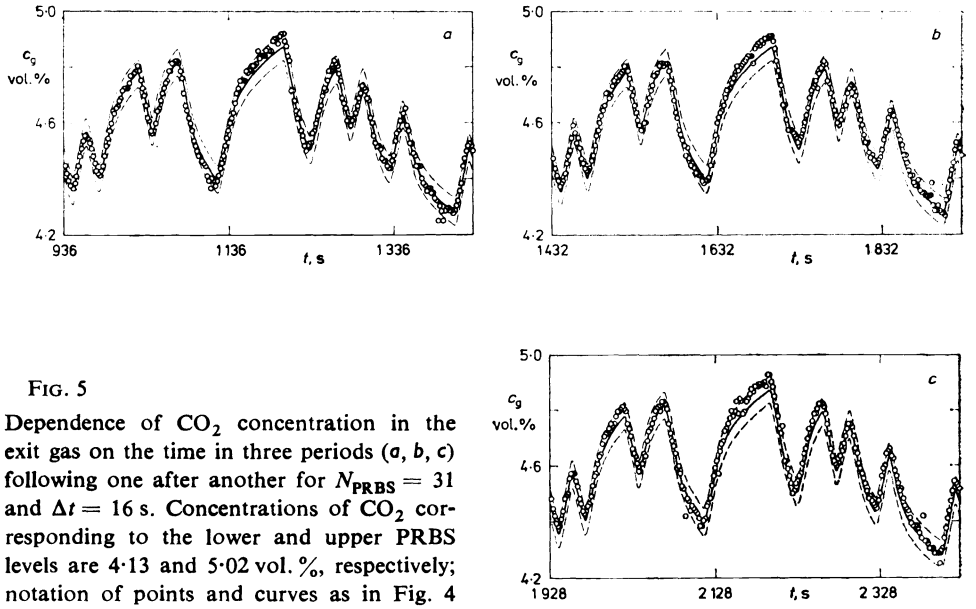

FIG. 5

Dependence of CO_2 concentration in the exit gas on the time in three periods (*a*, *b*, *c*) following one after another for $N_{PRBS} = 31$ and $\Delta t = 16$ s. Concentrations of CO_2 corresponding to the lower and upper PRBS levels are 4·13 and 5·02 vol. %, respectively; notation of points and curves as in Fig. 4

CONCLUSIONS

The responses of the bubble column as well as the impulse characteristics calculated from it are in good agreement with those obtained from the axial dispersion model with mass transfer. If the impulse characteristics in original and dimensionless coordinates are compared (Eqs (*15*) and (*16*)), it follows that the two representations are identical, hence the form of the impulse characteristic of the model does not change even when the driving force is very small. So the term in Eq. (*2*) corresponding to the mass transfer was analysed to determine the conditions under which both models become identical. It turned out that the model with mass transfer takes the form of the model without mass transfer for extremely low columns or for extremely high superficial velocities of the gas, or in the case where the system is in equilibrium. Hence, in identification experiments the driving force can be very small, limited from below only by the errors of measurements. This is especially advantageous for systems showing nonlinearities at larger input signal amplitudes. It can be concluded that the experimental method using PRBS is suitable for verification of the axial dispersion model of bubble column. The method can still be simplified and improved by measuring the input and output signals simultaneously and by choosing an analyser with a minimum time constant enabling the interval Δt_{PRBS} to be lowered, so that the resulting impulse characteristic in each Δt would be much less distorted.

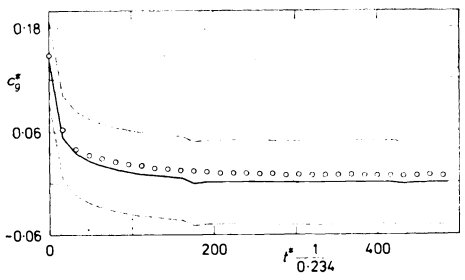

FIG. 6

Impulse characteristic found from the column response to an input PRBS with $N_{PRBS} = 31$, $\Delta t = 16$ s. The lower PRBS level corresponds to 4·13 vol. % of CO_2, the upper to 5·02 vol. % of CO_2; ——— calculated model impulse characteristic, ○ impulse characteristic determined from experimental data, — — — limits of errors

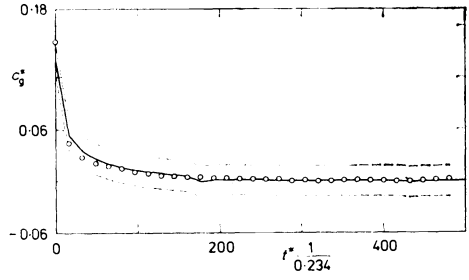

FIG. 7

Impulse characteristic found from the column response to an input PRBS with $N_{PRBS} = 31$, $\Delta t = 16$ s. Lower PRBS level corresponds to 1·22 vol. % of CO_2, upper to 5·17 vol. % of CO_2; notation of points and curves as in Fig. 6

LIST OF SYMBOLS

$\bar{a}$	coordinate of PRBS
a_l	interface area per unit volume of liquid, $m^2\ m^{-3}$
c	concentration, mol m^{-3}
D	dispersion coefficient, $m^2\ s^{-1}$
g_i	area delimited by ordinate of impulse characteristic and by time interval
$h(t)$	impulse characteristic
H	Henry constant, N m mol^{-1}
$k_{l(g)}$	mass transfer coefficients, m s^{-1}
L	height of bubble column, m
N	period of PRBS
$R_{xx}(j\Delta t)$	pseudocorrelation function of PRBS
$R_{xy}(j\Delta t)$	pseudocorrelation function of PRBS and system response
$R_{xN}(j\Delta t)$	pseudocorrelation function of PRBS and noise
$R_{xx}(\tau)$	autocorrelation function
$R_{xy}(\tau)$	crosscorrelation function
R	gas constant, kg $m^2\ s^{-2}\ mol^{-1}\ K^{-1}$
t	time, s
Δt	basic time interval of PRBS, s
T	temperature, K
U	real gas velocity, m s^{-1}
z	height coordinate, m
ε_g	gas hold-up
χ	linear equilibrium coefficient
τ	time shift

Subscripts

g	gas phase
l	liquid phase
*	dimensionless form
1	lower level of PRBS
2	upper level of PRBS

REFERENCES

1. Davies W. D. T.: Control, June, 302 (1966).
2. Davies W. D. T.: Control, July, 364 (1966).
3. Godfrey K. R.: Control, June, 305 (1966).
4. Culek A., Havel J., Přibyl V.: Kybernetika *2*, 215 (1966).
5. Peterka V.: Kybernetika *5*, 113 (1969).
6. Havlíček A.: *Thesis*. ÚTZCHT, ČSAV, Prague 1976.
7. Bischoff K. B., Levenspiel O.: Chem. Eng. Sci. *17*, 245 (1962).
8. Danckwerts P. V.: Chem. Eng. Sci. *2*, 1 (1953).
9. Himmelblau D. M., Bischoff K. B.: *Process Anlysis and Simulation*. Wiley, New York 1968.
10. Levenspiel O., Bischoff K. B.: Adv. Chem. Eng. *4*, 95 (1963).
11. Shah Y. T., Stiegel G. J., Sharma M. M.: AIChE J. *24*, 369 (1978).
12. Seher A., Schumacher V.: Ger. Chem. Eng. *2*, 117 (1979).

13. Diboun M., Schügerl K.: Chem. Eng. Sci. *22*, 147 (1967).
14. Hanratty T. J., Latinen G., Wilhelm R. H.: AIChE J. *2*, 372 (1956).
15. Schügerl K.: *Thesis.* Technical University, Hannover 1984.
16. Wen C. Y., Fan L. T.: *Models for Flow Systems and Chemical Reactors.* Dekker, New York 1975.
17. Afschar A. S., Diboun M., Schügerl K.: Chem. Eng. Sci. *23*, 253 (1968).
18. Pavlica R. T., Olson J. H.: Ind. Eng. Chem. *62*, 45 (1970).
19. Deckwer W. D.: Chem. Eng. Sci. *31*, 309 (1976).
20. Deckwer W. D., Adler J., Zaidi A.: Can. J. Chem. Eng. *56*, 43 (1978).
21. Mangartz K. H., Pilhofer T.: Chem.-Ing.-Tech. *50*, 693 (1978).
22. Mangartz K. H., Pilhofer T.: Presented at *6th CHISA Congress, Prague, August 21—25, 1978*; lecture F.4.5.
23. Serpemen Y., Deckwer W. D.: Ind. Eng. Chem., Fundam. *13*, 399 (1974).
24. Vašáková J.: *Thesis.* ÚTZCHT, ČSAV, Prague 1983.
25. Herles V.: Report No. 195, ÚTIA, ČSAV.
26. Zahradník J.: Collect. Czech. Chem. Commun. *44*, 348 (1979).
27. Kaštánek F., Zahradník J., Rylek M., Kratochvíl J.: Chem. Eng. Sci. *35*, 456 (1980).
28. Godfrey K. R., Murgatroyd W.: Proc. IEE *112*, 565 (1965).
29. Godfrey K. R., Everett D., Bryant P. R.: Proc. IEE *113*, 185 (1966).
30. Godfrey K. R.: Proc. IEE *113*, 1095 (1966).

Translated by K. Micka.